A Pilot-Carrier Coherent LEO-to-Ground Downlink System Using an Optical Injection Phase Lock Loop (OIPLL) Technique

Yozo Shoji, *Member, IEEE*, Martyn J. Fice, *Member, IEEE*, Yoshihisa Takayama, and Alwyn J. Seeds, *Fellow, IEEE*

***Abstract*—A pilot-carrier coherent low-earth-orbit (LEO) satellite to ground (LEO-to-Ground) downlink system using an optical injection phase lock loop (OIPLL) technique is proposed and its feasibility under Doppler frequency shift conditions is demonstrated. A fiber-optic based experimental system is configured and it is demonstrated that a 10 Gbps BPSK transmission system based on the proposed configuration can successfully maintain stable frequency and phase locking status under simulated Doppler frequency shift conditions. It is demonstrated that the stable locking status is maintained over a 10.3 GHz (54 ppm) frequency offset with a maximum rate-of-change of up to 32.4 GHz/s (168 ppm/s), which is ample to meet the requirement for a coherent LEO-to-Ground downlink system. The locking capability of the experimental system for more rapidly changing Doppler frequency shift is investigated. It is shown that the OIPLL receiver remains locked for maximum rates of change of 2.6 THz/s (13 500 ppm/s) or more for peak-to-peak frequency offsets up to 2 GHz (10.7 ppm). The phase noise performance of the system is also investigated and phase noise power of less than −100 dBc/Hz at greater than 1 MHz offset frequency is achieved even if the received laser signal suffers from a simulated Doppler frequency shift with peak-to-peak frequency offset of 2.4 GHz (12.5 ppm) and maximum rate of change of 750 GHz/s (3 900 ppm/s).**

***Index Terms*—Coherent, Doppler shift, downlink, laser, LEO, optical injection locking, optical phase lock loop (OPLL), satellite.**

I. Introduction

A phase-modulated optical communications system combined with a coherent homodyne detection technique brings advantages, such as greater receiver sensitivity, greater immunity to noise and interference, highly efficient use of optical frequency resource, and ability to demultiplex closely spaced WDM channels without optical filtering [1]–[4]. Thus, it has been considered a promising optical communications technique not only for fiber-optic communications, but also for free-space optical communications in space applications such as satellite-to-satellite links and satellite-to-ground links [5], [6].

The National Institute of Information and Communications Technology (NICT) in Japan has set the target of demonstrating the feasibility of a low-earth-orbit (LEO) satellite to ground downlink system which will allow enormous amounts of observation data to be downloaded from the LEO satellite [7]. Investigations to clarify the channel characteristics due to atmosphere propagation have been conducted [8] and optical amplifiers available for the space link have been developed targeting higher sensitivity [9]. However, the use of phase modulation technique has not been demonstrated yet due to a number of difficulties.

One of the difficulties inherent to a coherent LEO-to-Ground downlink system is that the receiver at an optical ground station (OGS) needs to be equipped with a local oscillator (LO) laser with frequency and phase precisely synchronized to the received laser signal. To compound the difficulty, a coherent LEO-to-Ground downlink system needs to cope with a critical Doppler frequency shift ranging over multiple gigahertz as described later.

One conventional solution for this synchronization issue has been integration of an optical phase-lock loop (OPLL) technique with the LO laser [10]–[12]. Yet it is known that the phase noise suppression effect obtained with this technique is limited due to the unavoidable loop propagation delay, and the laser linewidth used for the signal source must be comparatively narrow. Another solution is use of the optical injection locking (OIL) technique [13]–[15], which is known to offer an acceptable phase noise suppression effect with a realistic laser linewidth. However there is a drawback that the locking frequency range is limited to typically 1 GHz or less.

The digital coherent approach [16] which is now being deployed in fiber-optic networks could be another promising solution because the phase and frequency offset can be effectively estimated and compensated at the receiver by using high-speed digital signal processing (DSP) technology that has recently become available. However, the high power consumption of the DSP, and the cost of developing application-specific integrated circuits, may make a more conventional solution attractive in some situations.

The above discussion leads to the idea that use of an OPLL technique combined with an OIL technique, i.e., use of an optical injection phase-lock loop (OIPLL) technique [17]–[22], could be a suitable solution for the synchronization issue in a coherent LEO-to-Ground downlink system, where the LO laser

Manuscript received January 13, 2012; revised March 27, 2012; accepted April 30, 2012. Date of publication June 14, 2012; date of current version August 01, 2012. The work of Y. Shoji was supported by the Japan Society for the Promotion of Science (JSPS) through an Excellent Young Researchers Overseas Visit Program Fellowship.

Y. Shoji and Y. Takayama are with the National Institute of Information and Communications Technology, Tokyo 184-8795, Japan (e-mail: shoji@nict.go.jp; takayama@nict.go.jp).

M. J. Fice and A. J. Seeds are with the Department of Electronic and Electrical Engineering, University College London, London WC1E 7JE, U.K. (e-mail: m.fice@ucl.ac.uk; a.seeds@ucl.ac.uk).

Color versions of one or more of the figures in this paper are available online at http://ieeexplore.ieee.org.

Digital Object Identifier 10.1109/JLT.2012.2204037

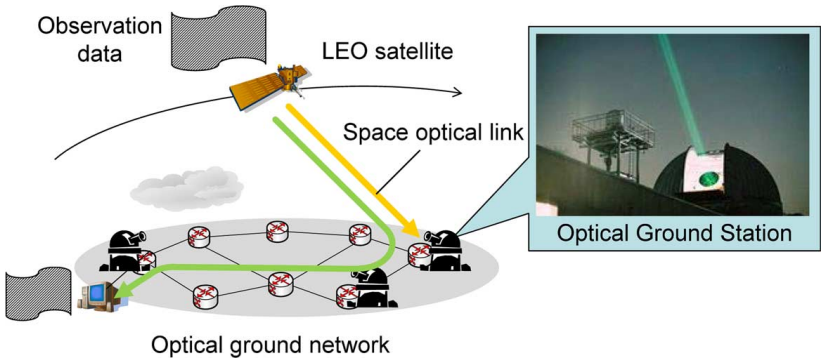

Fig. 1. Concept of a coherent LEO-to-Ground downlink system.

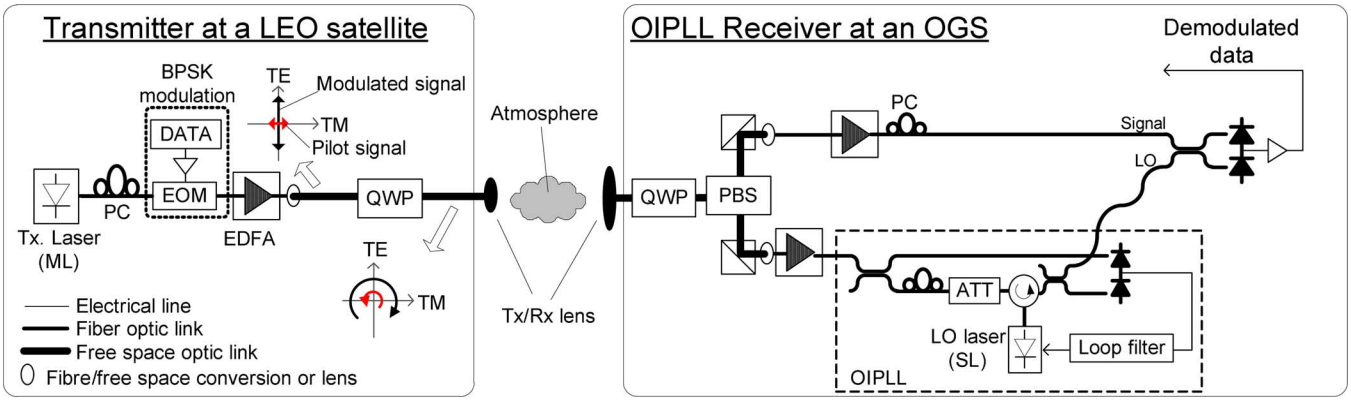

Fig. 2. Sample configuration of a pilot-carrier coherent LEO-to-Ground downlink system.

needs to remain stably frequency and phase locked to the received laser signal from a LEO satellite under severe Doppler frequency shift conditions. In addition, it is expected that the use of the OIPLL technique could relax the requirements on the linewidth and frequency stability of the transmitter laser installed in the satellite, which is exposed to extreme conditions in space.

This paper proposes and discusses a coherent LEO-to-Ground downlink system where a pilot carrier is transmitted along with a modulated signal in orthogonal polarizations in order to apply an OIPLL technique at the receiver. The rest of this paper is organized as follows. Section II describes the concept of a coherent LEO-to-Ground downlink system. Section III describes a sample configuration of a pilot-carrier coherent LEO-to-Ground downlink system. Section IV theoretically estimates Doppler frequency shift from which an LEO-to-Ground downlink should suffer. Section V details the experimental system configuration. Section VI shows the fundamental bit error ratio (BER) performance of the experimental system. Sections VII and VIII, respectively, show BER and phase noise performances of the experimental system under simulated Doppler shift conditions.

II. Concept of a Coherent LEO-to-Ground Downlink System

Fig. 1 illustrates the concept of a coherent LEO-to-Ground downlink system [23], where a LEO satellite is assumed to collect and store various kinds of observation data while orbiting. The collected data are transmitted to an optical ground station (OGS) while it is accessible by the LEO satellite. The received data at the OGS may be further transported to a data analysis station located in a remote place via ground networks as shown in Fig. 1.

A LEO satellite generally orbits at a height of hundreds of kilometers, moving at a velocity of several km/s. Consequently, the OGS needs to achieve highly accurate laser beam pointing [24] and must overcome signal fading due to atmospheric turbulence and clouds [7], [8], [25]. In addition, if a coherent communications technique is applied, the receiver at the OGS needs to cope with the frequency and phase synchronization issue under Doppler frequency shift conditions, where the frequency shift actually ranges over several gigahertz, as will be described in Section IV. Thus, we need to consider the tracking ability of the receiver carefully in developing a LEO-to-Ground downlink system.

III. A Sample Configuration of a Pilot-Carrier Coherent LEO-to-Ground Downlink System

Fig. 2 illustrates a sample configuration of a pilot-carrier coherent LEO-to-Ground downlink system. The proposed coherent system assumes optical pre-amplification at the receiver as shown in Fig. 2. Therefore, the receiver performance is dominated not by shot-noise but by beat-noise due to the local oscillator laser and amplified spontaneous emission (ASE) from the pre-amplifiers, i.e., LO-ASE beat noise.

The transmitter at the LEO satellite is equipped with a transmitter laser which works as a master laser (ML) and an external optical modulator (EOM) which modulates only the TE mode polarization light based on the applied voltage but passes the TM mode polarization light with no modulation. Consequently, if the laser signal at the input of the EOM is linearly polarized in a direction that is slightly inclined with respect to the modulation axis of the EOM, a modulated laser signal multiplexed with a CW orthogonal polarization pilot-carrier is obtained. The power ratio of the modulated signal and the pilot carrier can be controlled by adjusting the inclination angle using a polarization controller (PC).

Fortunately, it has been demonstrated that the polarization state is well maintained even after a laser signal propagates through the atmosphere in LEO-to-Ground downlink systems [26]. Thus, it is expected that the receiver can divide the pilot-carrier and the modulated signal with a high discrimination ratio by using a polarization beam splitter (PBS). However, since it would be difficult to estimate and match the directions of the linear polarization axis between the moving LEO satellite and the receiver at an OGS, the pilot-carrier and modulated laser signal should be multiplexed in circularly orthogonal polarizations, which can be achieved by inserting a quarter-wave plate (QWP) in the front end of both the transmitter and receiver, as shown in Fig. 2.

The OIPLL receiver at an OGS first divides the received light into modulated signal and pilot-carrier using a PBS. The extracted pilot-carrier power is further divided into two parts, one of which is injected into a slave laser (SL) after polarization and power adjustments, while the other part is used for phase-error detection. Most of the output power from the SL is used as a local oscillator (LO) signal for coherent detection of the data, but some is mixed with the received pilot-carrier and photo-detected to generate a phase-error signal as shown in Fig. 2. The phase-error signal is used to control the frequency and phase of the SL. The scheme illustrated in Fig. 2 shows the modulated signal and LO being combined in a simple coupler, allowing demodulation of data in a single quadrature. However, a 90-degree optical hybrid could be used instead, allowing recovery of both in-phase and quadrature-phase components of the modulated data signal.

Essential for the operation of any satellite communications system are the acquisition and tracking sub-systems. First, mechanical laser pointing to establish the connection must be carried out, which in a LEO-to-Ground link generally takes several seconds [5], [6]. Exact frequency and phase locking by the OIPLL has been demonstrated to take less than 10 ns [22], once the input signal falls within the optical injection locking range. However, stable locking requires a low optical injection ratio, resulting in a narrow locking range of around 1 GHz [21]. It would therefore be necessary to tune the free-running frequency of the LO laser until it matches that of the Doppler-shifted signal laser. We envisage that the LO laser's frequency could be scanned over the range corresponding to the Doppler-shifted signal until injection locking is detected, then the slow PLL tracking loop turned on to bring the LO frequency to the center of the locking range and to track the changing Doppler shift. Since rapid tuning of the LO laser is possible (on a millisecond timescale or quicker), this should be a rapid process. The initial mechanical alignment process is therefore expected to dominate the overall acquisition time.

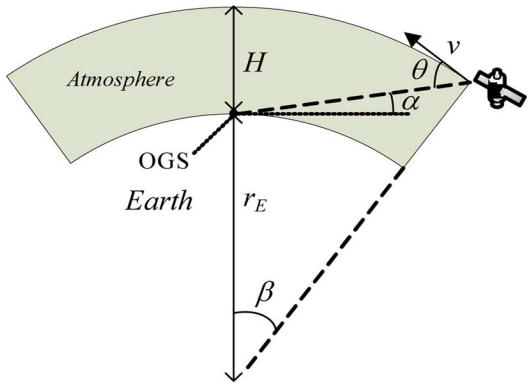

Fig. 3. Simplified moving model for a LEO-to-Ground downlink.

Once the signal has been acquired, the slow PLL loop will track the Doppler-shifted signal frequency and ensure operation at the center of the optical injection locking range. In the event of a signal fade, automatic gain control in the optical amplifiers should maintain the injected signal power at an approximately constant value, preventing locking being lost except in the case of very deep fades. In the event that locking is lost, the frequency scanning acquisition process would have to be restarted until adequate power for locking is once again achieved. Provided spatial tracking is not also lost, it should be possible to re-establish communications very rapidly after a fade.

Although these acquisition processes should be conducted automatically in a practical system, we carried them out manually in the experiments described in the rest of this paper.

IV. Theoretical Estimation of Doppler Frequency Shift for a Coherent LEO-to-Ground Downlink

A. Moving Model for a LEO Satellite

A moving model of a LEO satellite can be simplified as shown in Fig. 3, where the earth is assumed to be a perfect sphere. α is the LEO satellite's elevation angle when viewing it from the OGS point, r_E is the earth's radius, H is the orbit's altitude, and β is the angle indicating the LEO satellite position relative to the zenith position.

The Doppler frequency shift, f_D, can be expressed as follows [27]:

$$f_D = f_c \left(\frac{\sqrt{1 - \frac{v^2}{c^2}}}{1 - \frac{v}{c}\cos\theta} - 1 \right) \tag{1}$$

where c and f_c are the velocity of light and the center frequency of the transmitted laser signal, respectively. v is the velocity of the LEO satellite which can be expressed by

$$v = \sqrt{\frac{\mu_G}{r_E + H}} \tag{2}$$

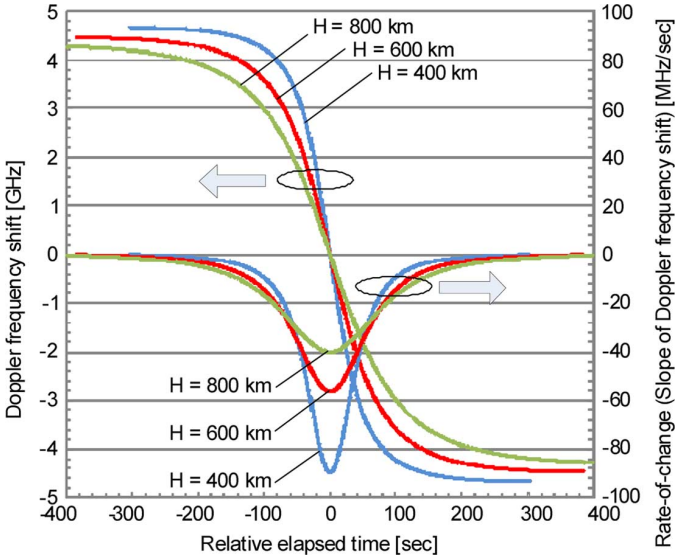

Fig. 4. Doppler frequency shift and rate-of-change versus relative elapsed time.

TABLE I
PARAMETERS USED FOR DOPPLER EFFECTS ANALYSIS

Symbol	Parameters	Values
λ	Wavelength of the Master Laser	1566 nm
r_E	Radius of Earth	6357 km
H	Height of LEO satellite	400/600/800 km
μ_G	Gravitational constant times mass of Earth	3.986×10^{14} $\mathrm{m}^3/\mathrm{s}^2$

where μ_G is the gravitational constant multiplied by the mass of the Earth. θ is the angle determined by α and β as follows.

$$\theta = \alpha + \beta = \arccos\left(\frac{r_E}{r_E + H} \cdot \cos\alpha\right) \tag{3}$$

$$\beta = \arccos\left(\frac{r_E}{r_E + H} \cdot \cos\alpha\right) - \alpha. \tag{4}$$

Using β, the relative elapsed time, τ, is expressed by,

$$\tau = (r_E + H) \cdot \frac{\beta}{v}. \tag{5}$$

B. Numerical Estimation of Doppler Frequency Shift for a Coherent LEO-to-Ground Downlink

Fig. 4 shows the Doppler frequency shift versus relative elapsed time when the example parameters listed in Table I are used. We can see from this figure that the Doppler frequency shift ranges from approximately -4.5 GHz to $+4.5$ GHz, which means the receiver for the LEO-to-Ground downlink is required to have a locking capability over a frequency range of at least 9 GHz. Another important factor in considering the required locking capability of the receiver is the rate-of-change, i.e., the slope of the Doppler frequency shift. Fig. 4 also shows the rate-of-change versus relative elapsed time for the three different heights of LEO satellite. We can see from the figure that the lower height causes a more rapid change of the Doppler frequency shift. If we take the absolute value of the rate-of-change, the maximum rate-of-change were 90 MHz/s, 56 MHz/s, and 40 MHz/s for heights of 400 km, 600 km, and 800 km, respectively.

V. CONFIGURATION OF FIBER-OPTIC BASED EXPERIMENTAL SYSTEM

In order to demonstrate the feasibility of the coherent LEO-to-Ground downlink system described in Section III, a fiber-optic based experimental system was configured as shown in Fig. 5. Table II lists the main parameters of the experimental system. For simplicity, BPSK modulation was used.

The system configuration is almost the same as that shown in Fig. 2. However, all the components and the transmission link are configured using only fiber-pigtailed components. In addition, linear orthogonal polarizations are used to multiplex the pilot-carrier with modulated signal at the transmitter.

As shown in Fig. 5, the experimental system can be divided into three parts: transmitter, transmission link, and OIPLL receiver. The transmitter part consisted of a distributed feedback (DFB) laser diode which works as a master laser (ML), a GaAs-based Mach–Zehnder modulator (MZM), a polarization controller (PC), and a transmitter erbium-doped fiber amplifier (EDFA) to boost the transmission power. The MZM was specially designed to transmit both TE and TM polarized fields with low loss but with only the TE polarized field modulated according to the applied voltage. This feature enables us to transmit a TE polarized laser signal modulated with BPSK format along with a TM polarized pilot-carrier [21].

The power ratio of the modulated signal and pilot-carrier was 5:1 (7 dB) in our experimental demonstration, giving a power penalty of only 0.8 dB due to the unmodulated power in the pilot-carrier.

The Doppler frequency shift of the transmitted laser signal was simulated by directly modulating the ML drive current with a sinusoidal signal generated by a function generator (FG). Fig. 6 illustrates how the ML's frequency was deviated in the experiment. The applied signal's amplitude and frequency were adjusted to simulate a Doppler frequency shift with the required target peak-to-peak frequency offset (ΔF) and deviation rate (F_R), using the measured DC frequency modulation sensitivity of the ML for calibration.

The simulated Doppler frequency shift, f_D, and the normalized one, f'_D are expressed by,

$$f_D = \frac{\Delta F}{2}\sin(2\pi F_R t) \tag{6}$$

$$f'_D = \frac{\Delta F}{2f_c}\sin(2\pi F_R t) \tag{7}$$

where f_c is the ML's center frequency.

From (6) and (7), the maximum rate-of-change of the simulated Doppler frequency shift, $S_{\max}$, and the normalized one, $S'_{\max}$, can be expressed as follows:

$$\begin{aligned} S_{\max} &= \max\left[\frac{df_D}{dt}\right] \\ &= \max\left[\pi F_R \Delta F \cos(2\pi F_R t)\right] \\ &= \pi F_R \Delta F \end{aligned} \tag{8}$$

$$S'_{\max} = \pi F_R \cdot \frac{\Delta F}{f_c}. \tag{9}$$

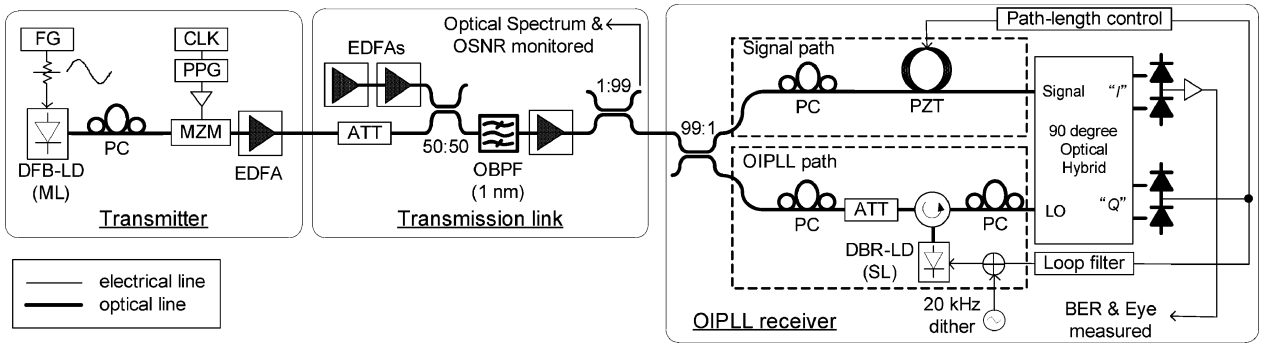

Fig. 5. Experimental system to test coherent link performance under simulated Doppler frequency shift conditions.

TABLE II
MAIN PARAMETERS OF EXPERIMENTAL SYSTEM

Parameters	Values
Wavelength of the Master Laser (ML)	1566 nm
Output power of the transmitter	7 dBm
Injection Ratio for the Slave Laser (SL)	About -40 dB
Modulation scheme	BPSK
Data rate	10 Gbps
PRBS pattern	$2^{31}-1$
Linewidth of free running ML (FWHM)	1.5 MHz
Linewidth of free running SL (FWHM)	1.0 MHz
Modulated signal to pilot-carrier power ratio	5:1

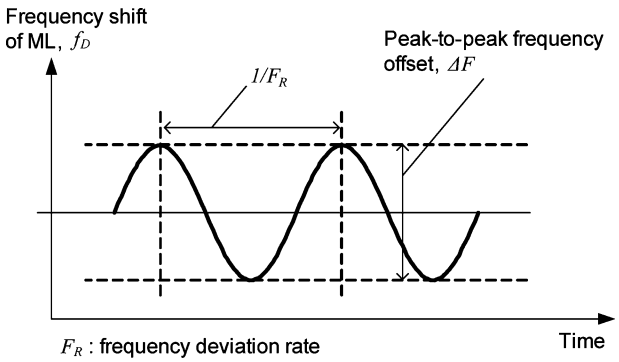

Fig. 6. How the Master Laser (ML) frequency was deviated.

The DC frequency modulation sensitivity of the ML was approximately 680 MHz/mA, allowing a peak-to-peak frequency offset greater than 10 GHz to be achieved by applying approximately 15 mA peak-to-peak current variation about the mean bias current of 50 mA. Although the direct modulation of the ML to simulate Doppler frequency shift also causes the change of the ML output power, we experimentally confirmed that automatic output power control of the transmitter EDFA reduces power fluctuation at the transmitter output to less than 0.5 dB when F_R is less than 500 Hz, even for $\Delta F = 10$ GHz.

As described in Section III, the OIPLL receiver is assumed to operate under LO-ASE beat-noise limited conditions. Thus, the operation of the OIPLL receiver and the data transmission performance were investigated for several optical signal-to-noise ratio (OSNR) conditions, which were simulated by using erbium doped fibre amplifiers (EDFAs) as illustrated in the transmission link part of Fig. 5.

The transmission link transferred the transmitted laser signal to the OIPLL receiver with a specified OSNR and a specific power level. The OSNR is defined as the ratio of the optical signal power to the optical noise power in an optical bandwidth of 0.1 nm. The transmitted laser signal was combined with ASE noise from a two-stage EDFA, filtered using a 1 nm bandwidth optical bandpass filter, and further amplified by another EDFA. 1 percent of the output power of this final stage EDFA was tapped off to monitor the optical spectrum and OSNR as shown in Fig. 5. To obtain the OSNR at the signal wavelength, the noise power was measured at an offset of 0.25 nm from the signal peak wavelength and corrected to account for the filter shape.

The OSNR can be translated into the received optical power or photons/bit if the noise figure (NF) of the receiver amplifier is known. For example, an OSNR of 5 dB is calculated to correspond to a received power of about -48 dBm, assuming that the NF of the preamplifier is 5 dB.

The OIPLL receiver consisted of an optical coupler to tap off some of the received laser signal to injection lock a slave laser (SL), a distributed Bragg reflector (DBR) laser diode (the SL), a $LiNbO_3$-based integrated optical hybrid, and two pairs of balanced photo detectors (PDs). Three manually controllable PCs, an optical variable attenuator (ATT), and an optical circulator were respectively implemented for matching of laser signal polarizations, for obtaining the required injected laser signal power at the SL, and to separate the SL output from the injection path.

When the transmitter was adjusted to give BPSK-modulated data and the SL was locked to the ML, the two outputs of the optical hybrid gave demodulated baseband data and a phase-error signal, respectively. The phase-error signal was fed back to control the drive current of the SL via a suitable loop filter, forming an OPLL.

There were two paths between the optical input coupler and the optical hybrid; the signal path and the OIPLL path, as shown in Fig. 5. The OIPLL receiver was constructed from fiber-pigtailed components and consequently the path length from the input coupler to the SL and on to the input of the optical hybrid was several meters. To ensure that the relative phase of the inputs to the optical hybrid remained constant, the length of the signal path was actively controlled using a piezo-electric fibre stretcher (PZT). The error signal for this control loop was derived by directly modulating the SL with a 20 kHz dither at low modulation index.

Further details of the experimental OIPLL receiver can be found in [21].

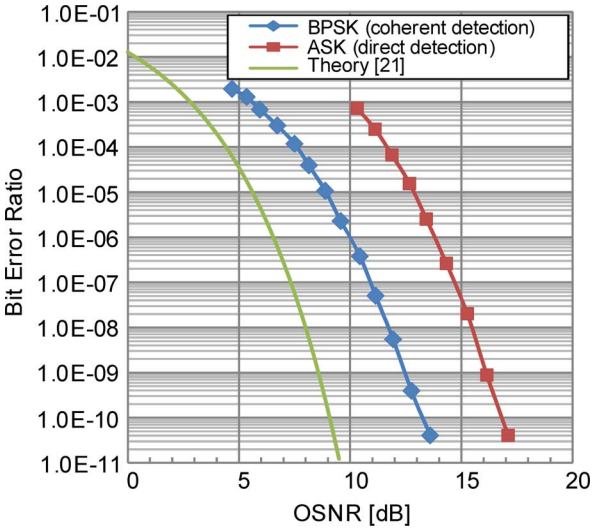

Fig. 7. Fundamental BER performances versus OSNR (no Doppler frequency shift).

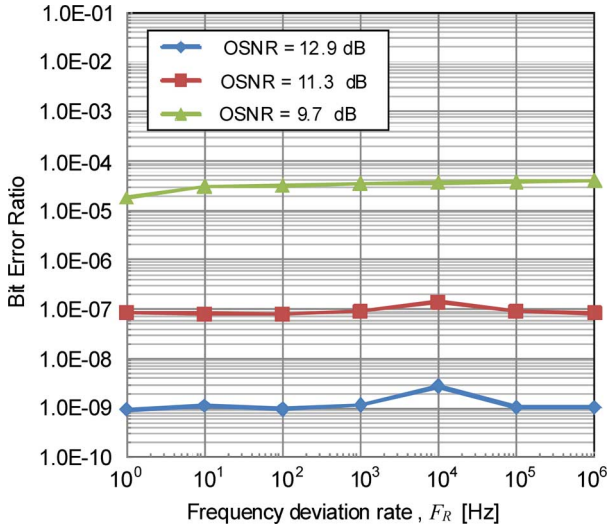

Fig. 8. Bit error rate versus frequency deviation rate [ΔF = 206 MHz (1.1 ppm)].

VI. Fundamental BER Performance of the Experimental System

Fig. 7 shows the fundamental BER performance of the experimental system for different OSNR conditions when no Doppler frequency shift is simulated.

For comparison, this figure also includes the theoretical ideal BER performance for coherent BPSK detection [21] and the BER performance when a binary amplitude shift keying (ASK) signal was transmitted without pilot carrier and directly detected. The binary ASK modulation was accomplished by changing the bias voltage applied to the MZM.

It was observed that error-free performance ($\mathrm{BER} \leq 10^{-11}$) was obtained with an OSNR of over 14.5 dB for coherent detection of BPSK, and over 18 dB for direct detection of ASK. About 3.5 dB reduction in OSNR was achieved by using coherent detection of BPSK signal at $\mathrm{BER} = 10^{-5}$ compared to direct detection of the ASK signal. Compared to the theoretical performance, it was observed that the experimental BPSK system suffers a penalty of 3 dB or more. 0.8 dB of the penalty should be due to the orthogonal pilot as described in Section V, while the other penalty is attributed mainly to the non-optimal electrical filtering with bandwidth of approximately 10 GHz.

A practical LEO-to-Ground link suffers severe loss due to atmosphere propagation and the received power could be less than -30 dBm or sometimes less than -40 dBm [7]. As explained above, an OSNR of 5 dB is calculated to correspond to a received power of -48 dBm. Since the SL remains locked when the OSNR is about 4.5 dB, as shown in Fig. 7, we can conclude that the system can work with the very low received power condition which could happen due to scintillation in general LEO-to-Ground optical links.

The prior works in [2] and [3] report uncoded sensitivities at 10^{-9} BER that were 4.4 dB and 3.5 dB higher than the shot-noise limit, for a 2 Mbps PSK system and a 312 Mbps PSK system, respectively. Our experimental 10 Gbps PSK system achieved 10^{-9} BER with the OSNR of about 12.5 dB, a 4 dB penalty compared to the LO-ASE limit relevant to our optically pre-amplified system. Thus, we have achieved a similar implementation penalty, but at a much higher bit rate. In addition, this performance can be achieved under a wide Doppler frequency shift condition as described later in Section VII.B.

Fig. 7 shows that a stable locking status with the BER of 0.002 was obtained when the OSNR was about 4.5 dB. Coding techniques [2], [3] allow virtually error-free performance to be achieved under conditions corresponding to OSNR lower than this. Operation of the OIPLL receiver in this regime will be investigated and reported later.

VII. BER Performance of the Experimental System Under Simulated Doppler Frequency Shift Conditions

A. Impact of Narrow Doppler Frequency Shift Conditions

Fig. 8 shows the BER performances versus frequency deviation rate, F_R, when the received laser signal suffers from simulated Doppler frequency shift for three different OSNR conditions, and where the peak-to-peak frequency offset, ΔF, is fixed at about 206 MHz (1.1 ppm).

The phase difference, θ_0, between two injection-locked lasers varies according to the difference between the free-running frequencies of the lasers (f_d) as follows [15]:

$$f_d = \frac{B_{\mathrm{OIL}}}{2} \sin(\theta_0 - \tan^{-1} \alpha_{\mathrm{SL}}) \tag{10}$$

where B_{OIL} is the full injection locking range and α_{SL} is the linewidth enhancement factor of the SL. This phase error should be tracked and compensated by the OPLL control as long as the deviation rate is lower than the bandwidth over which the electronic PLL dominates the overall response of the OIPLL (about 1 kHz).

Assuming the injection locking range is 1 GHz, we can estimate from (10) that the amplitude of the phase variation is only about 12 degrees, which would not give significant impact on the BER performance unless we evaluate it at very high OSNR conditions. Therefore, we can see from Fig. 8 that the BER

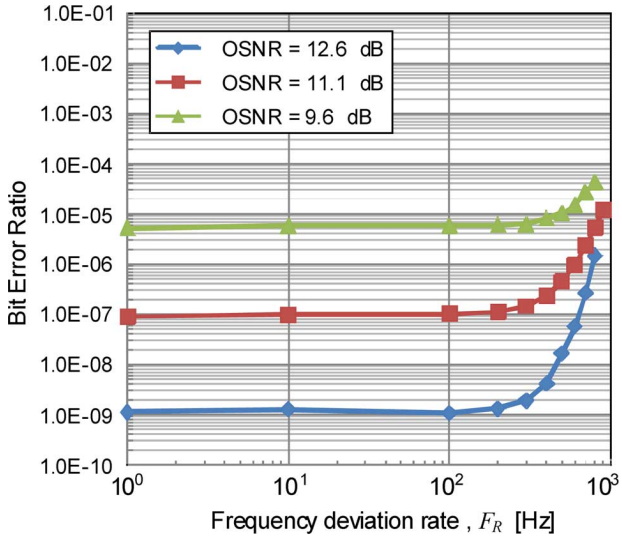

Fig. 9. Bit error rate versus frequency deviation rate [ΔF = 1031 MHz (5.4 ppm), BER was measured until the receiver unlocked].

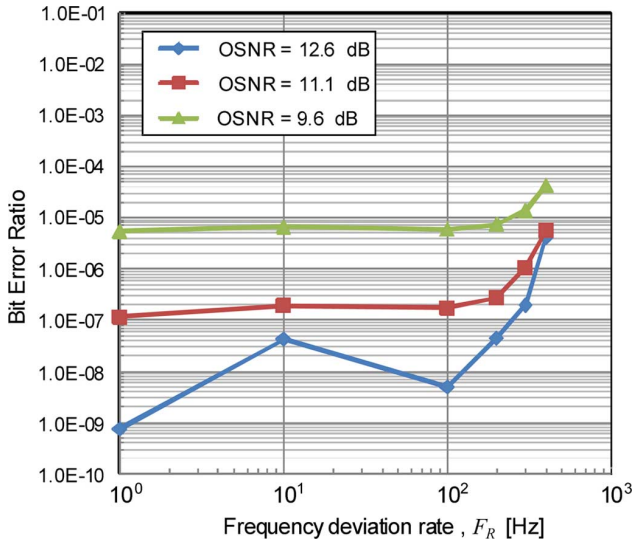

Fig. 10. Bit error rate versus frequency deviation rate [ΔF = 2063 MHz (10.7 ppm), BER was measured until the receiver unlocked].

remains approximately constant, even at deviation rates much higher than the bandwidth of the electrical loop of the OPLL.

Figs. 9 and 10 also show the BER performances versus the frequency deviation rate for three different OSNRs, where the peak-to-peak frequency offset, ΔF, is fixed at 1031 MHz (5.4 ppm) and 2063 MHz (10.7 ppm), respectively.

We can see from these figures that the BER remained approximately constant until the deviation rate reached a certain threshold deviation rate. As the deviation rate was increased beyond the threshold rate, the BER increased, with the receiver eventually becoming unlocked.

We observe from Figs. 9 and 10 that the BER performance degraded more rapidly after the deviation rate exceeded the threshold rate for the wider peak-to-peak frequency offset, and the receiver became unlocked at a lower deviation rate. For example, we can see that the BER for the condition of OSNR = 12.6 dB is degraded to 10^{-7} at a deviation rate of

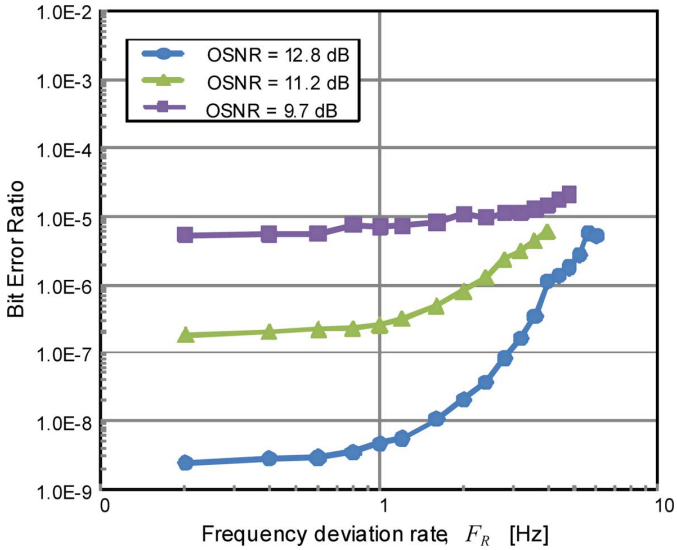

Fig. 11. BER performances versus frequency deviation rate, F_R.[ΔF = 10.3 GHz (54 ppm), BER was measured until the receiver unlocked].

600 Hz for the deviation range of 1031 MHz (see Fig. 9), while a deviation rate of about 250 Hz results in the same degradation when the peak-to-peak frequency offset is 2063 MHz (see Fig. 10).

The receiver became unlocked at a deviation rate of around 800 Hz and 400 Hz in our experimental system for the peak-to-peak frequency offset of 1031 MHz (5.4 ppm) and 2063 MHz (10.7 ppm), respectively. Since the OPLL control suppresses phase variations in inverse proportion to the frequency deviation rate in the electronic control region, the same residual phase error amplitude would be expected at $F_R = 800$ Hz with $\Delta F = 1031$ MHz as at $F_R = 400$ Hz with $F_R = 2063$ MHz, which corresponds to conditions required to generate the maximum rate-of-change of the simulated Doppler frequency shift, $S_{\max}$, of 2.59 THz/sec (13 500 ppm/s).

It can be deduced from these results that the capability of the OIPLL receiver to track the frequency shift of the received signal is roughly limited by the maximum rate-of-change of the simulated Doppler frequency shift when the peak-to-peak frequency offset is greater than the injection-locking bandwidth (i.e., when locking is maintained by the electronic feedback), while much more rapid tracking ability is possible when the peak-to-peak frequency offset is less than the injection locking bandwidth (i.e., when locking is maintained by optical injection locking).

B. Impact of Wide Doppler Frequency Shift Conditions

Fig. 11 shows the BER performance when the received laser signal suffers from simulated Doppler frequency shifts for different frequency deviation rates, F_R, in which the peak-to-peak frequency offset, ΔF, is fixed at about 10.3 GHz (54 ppm). Three BER performances for different OSNR conditions are shown together: OSNR = 12.8, 11.2, and 9.7 dB.

From the previous discussions, we may expect that the OIPLL receiver should remain locked until the frequency deviation rate reaches 80 Hz for a peak-to-peak frequency offset of 10.3 GHz, corresponding to $S_{\max} = 2.59$ THz/sec. However, we can see

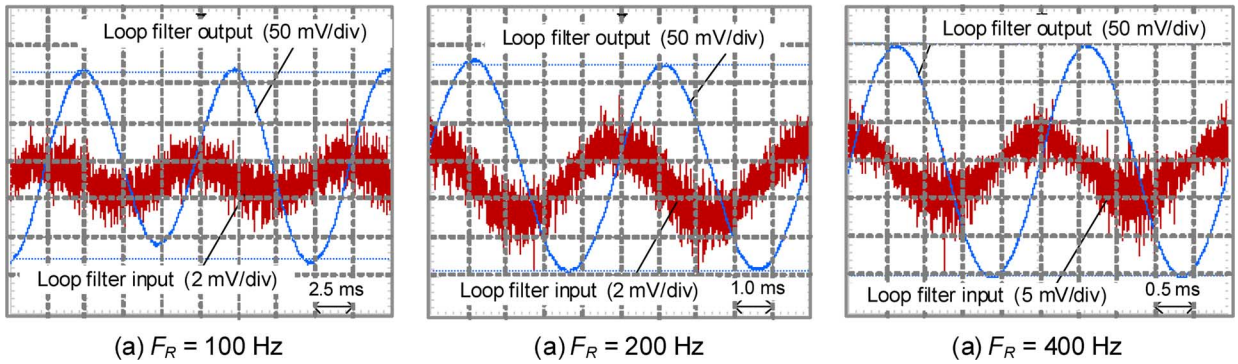

Fig. 12. Waveforms of loop filter input and output in the PLL circuit for different deviation rate of $F_R[\Delta F = 2063$ MHz (10.7 ppm)].

from Fig. 11 that the receiver became unlocked for all cases at less than 10 Hz deviation rate.

This discrepancy might be due to the behavior of the thermal controller circuit for the SL which was not independent of the injected frequency, especially when the deviation rate is very slow and the frequency offset large. We observed that the thermal control current was changing when the signal frequency was changing slowly. The change of the temperature will also affect the frequency of laser, and may cause the loop to become unstable at a lower deviation rate than expected.

Even so, as far as slow deviation rate up to 1 Hz is concerned, we can see that stable phase locking is maintained and almost no BER degradation is observed despite the receiver experiencing a large simulated Doppler frequency shift of over 10 GHz peak-to-peak frequency offset. Note that the 10.3 GHz peak-to-peak frequency offset at 1 Hz deviation rate results in a maximum rate-of-change of 32.4 GHz/s (168 ppm/s).

VIII. Phase Error and Phase Noise Performance of OIPLL Receiver Under Simulated Doppler Frequency Shift Conditions

Monitoring the input and output of the loop filter in the PLL circuit provides useful information to understand the behavior of the phase-lock loop. Fig. 12 shows the waveforms of the loop filter input and output for different frequency deviation rates of $F_R = 100$ Hz, 200 Hz, and 400 Hz, when the peak-to-peak frequency offset is fixed at 2063 MHz (10.7 ppm).

The loop filter output waveforms, which control the drive current of the SL, are depicted in blue lines, while the loop filter input waveforms, which indicate the amount of the phase error, are depicted in red lines.

We can see in Fig. 12 that stable sinusoidal PLL control signals are provided from the loop filter output with an amplitude of 250 $\mathrm{mV_{pp}}$ - 300 $\mathrm{mV_{pp}}$ for all the frequency deviation rate conditions. However, the observed amplitudes of residual phase error at the loop filter input differ considerably for different deviation rate conditions. For a deviation rate of 100 Hz, the peak-to-peak variation of the underlying sinusoidal phase error signal was about 2 $\mathrm{mV_{pp}}$, while for deviation rates of 200 Hz and 400 Hz, this increased to about 4 $\mathrm{mV_{pp}}$ and 8 $\mathrm{mV_{pp}}$, respectively.

It can be deduced that this significant increase of phase error is the immediate reason for the degradation of BER performance for the higher frequency deviation rates. The peak-to-peak frequency offset in this example, i.e., $\Delta F = 2063$ MHz, is much greater than the injection locking bandwidth (around 1 GHz). Therefore, it is believed that the locking performance is basically dominated by the performance of the OPLL circuit and the receiver becomes unlocked once the deviation rate exceeds the capability of the OPLL circuit.

In order to investigate the phase noise performance of the experimental optical transmission system, a TE polarized signal phase-modulated with a 5 GHz subcarrier was transmitted along with a TM polarized pilot carrier in a similar way to the previous BPSK signal transmissions. The OIPLL receiver was locked to the received TM polarized pilot carrier, allowing the 5 GHz subcarrier to be demodulated. The phase noise performance of the detected 5 GHz subcarrier was measured using a spectrum analyzer in order to assess the phase error introduced by the OIPLL receiver.

Figs. 13 and 14 respectively show the spectrum and phase noise performance of the original 5 GHz modulation signal and the coherently detected signal when no Doppler frequency shift is applied. It was observed that the phase noise of the coherently detected signal is degraded by about 10 dB at the frequency offset of up to 100 kHz, and by about 5 dB at the frequency offset of more than 100 kHz. However, phase noise of less than -110 dBc/Hz was achieved at the frequency offset of 1 MHz after the optical transmission. Note that the sharp peak in the phase noise spectrum at 20 kHz frequency offset in Fig. 14 is caused by the phase modulation used for controlling the fiber path length as described in Section V.

Fig. 15 shows sample phase noise performances after optical transmission when simulated Doppler frequency shifts are applied for different frequency deviation rates, F_R, and the peak-to-peak frequency offset is fixed at about 2.4 GHz. The figure shows that the phase noise performance at frequencies above 100 kHz degrades slightly as the deviation rate increases. Even so, phase noise of less than -100 dBc/Hz was achieved for all simulated conditions at ≥ 100 kHz offset.

At lower offset frequencies, less than 20 kHz, the phase noise is seen to increase over a bandwidth that scales with the frequency deviation rate (from approximately 200 Hz at $F_R = 1$ Hz to 20 kHz at $F_R = 100$ Hz). Similar spectra were observed even when direct detection of the frequency-modulated master signal was performed using the OIPLL receiver. These features

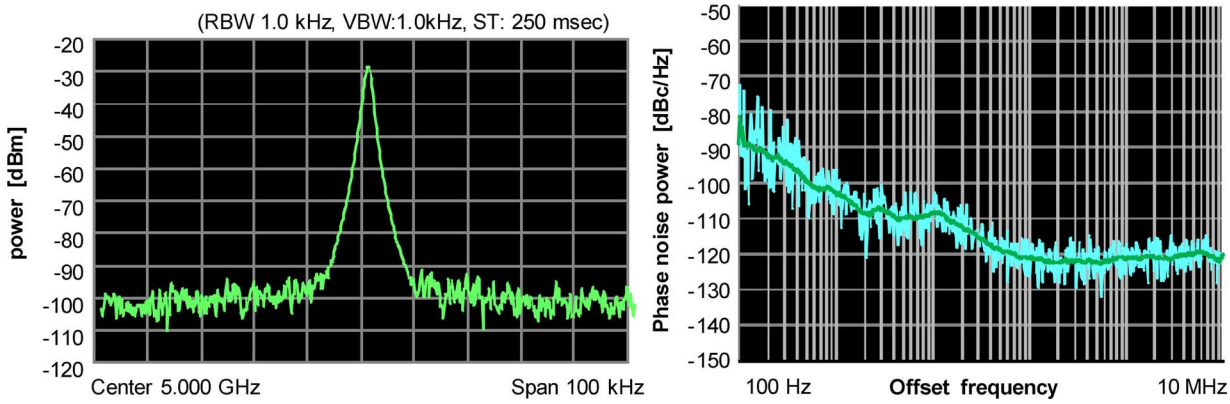

Fig. 13. Spectrum and phase noise performance of original 5 GHz modulation signal.

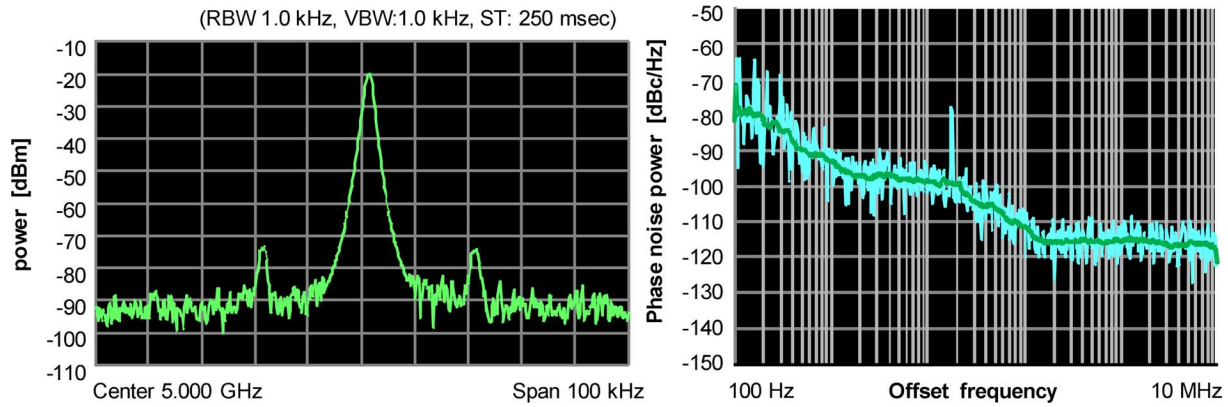

Fig. 14. Spectrum and phase noise performance of coherently detected 5 GHz signal.

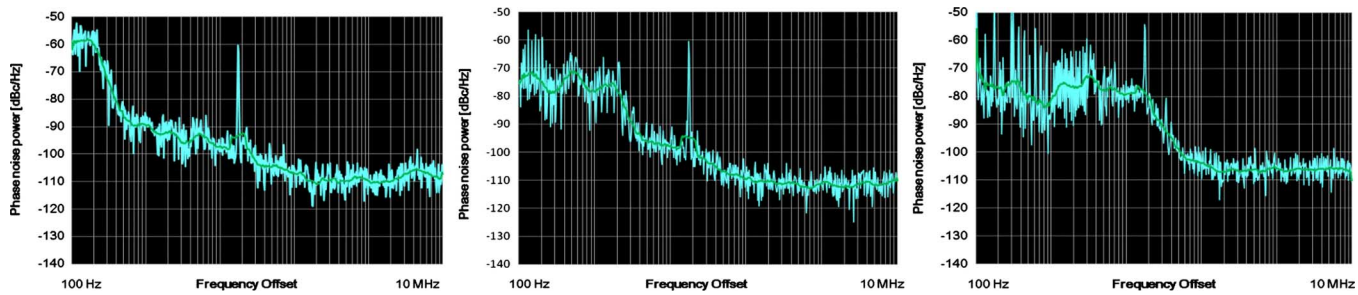

Fig. 15. Examples of phase noise of coherently detected 5 GHz signal for ML with simulated Doppler frequency shift [$\Delta F = 2.4$ GHz (12.5 ppm)] (left: $F_R = 1$ Hz, middle: $F_R = 10$ Hz, right: $F_R = 100$ Hz)

of the spectra are believed to be related to low-level reflections in the receiver, resulting in multiple signal paths.

Overall, from these results we conclude that the phase-tracking performance of the receiver is not significantly degraded even when the center frequency of the received laser signal varies over a wide frequency offset (a few GHz) and at high rate-of-change ($S_{\max} = 750$ GHz/s (3 900 ppm/s) or more).

IX. Conclusion

This paper proposed the concept and configuration of a pilot-carrier coherent LEO-to-Ground downlink system using an OIPLL technique and it was demonstrated that the receiver can maintain a stable frequency and phase locking state under simulated Doppler frequency shift conditions.

The peak-to-peak frequency offset and the maximum rate-of-change of the Doppler frequency shift that are expected to occur in a LEO-to-Ground downlink system were theoretically studied and estimated as greater than 9 GHz (47 ppm) and less than 100 MHz/s (0.5 ppm/s), respectively.

The BER and phase noise performances of the proposed system under simulated Doppler frequency shift conditions were experimentally investigated by configuring an equivalent experimental system of the pilot-carrier coherent LEO-to-Ground downlink system using fiber-pigtailed components.

The locking capability of the experimental system for comparatively narrow Doppler frequency shift conditions was first investigated. The OIPLL receiver did not become unlocked even at a deviation rate of more than 10 MHz for a peak-to-peak frequency offset of 206 MHz, while the re-

ceiver lost lock at deviation rates of 800 Hz and 400 Hz for the peak-to-peak frequency offset of 1031 MHz (5.4 ppm) and 2063 MHz (10.7 ppm), respectively. These conditions at which the receiver became unlocked correspond to a maximum rate-of-change of Doppler frequency shift of 2.59 THz/sec (13 500 ppm/s). Thus, it is concluded that the maximum capability of the OIPLL receiver is limited by a constant which is proportional to the peak-to-peak frequency offset times the deviation rate unless the peak-to-peak frequency offset is much narrower than the injection locking range. The tracking capability of the receiver is limited by the frequency range over which the electronic feedback operates and the slew rate of the electronic circuits. It is expected that faster electronic feedback circuits could be developed that would allow tracking of wider frequency deviation and higher rate of change of frequency.

It was also successfully demonstrated that the experimental system can maintain stable frequency and phase locking state with no power penalty for detection of a 10 Gbps BPSK signal under a simulated Doppler frequency shift condition over a 10.3 GHz (54 ppm) frequency offset with a maximum rate-of-change of up to 32.4 GHz/sec (168 ppm/s).

Since our immediate target was to investigate the feasibility of the proposed pilot-carrier coherent LEO-to-Ground downlink system under a Doppler frequency shift condition where the peak-to-peak frequency offset is greater than 9 GHz (47 ppm) and the maximum rate-of-change is less than 100 MHz/s (0.5 ppm/s), the performance of the experimentally investigated system is found to be more than sufficient to meet the requirements.

The phase noise performance of the transmitted signal was also investigated under simulated Doppler frequency shift conditions. At a frequency offset of 1 MHz, the phase noise power of less than -110 dBc/Hz was achieved without simulated Doppler frequency shift, and less than -100 dBc/Hz under a simulated Doppler frequency shift condition of 2.4 GHz (12.5 ppm) peak-to-peak frequency offset and deviation rate of up to 100 Hz.

ACKNOWLEDGMENT

The experimental work described in this paper was carried out while Y. Shoji was a visiting researcher at University College London.

REFERENCES

[1] K.-P. Ho, *Phase-Modulated Optical Communication System*. Berlin, Germany: Springer, 2005.

[2] B. Wandernoth, "5 Photon/bit low complexity 2 Mbit/s PSK transmission breadboard experiment with homodyne receiver applying synchronization bits and convolutional coding," in *Proc. Eur. Conf. Opt. Commun.*, 1994, vol. 1, pp. 59–62.

[3] M. L. Stevens, D. O. Caplan, B. S. Robinson, D. M. Boroson, and A. L. Kachelmyer, "Optical homodyne PSK demonstration of 1.5 photons per bit at 156 Mbps with rate 1/2 turbo coding," *Opt. Exp.*, vol. 16, no. 14, pp. 10412–10420, Jun. 2008.

[4] S. Kaneko, H. Suzuki, N. Miki, H. Kimura, and M. Tsubokawa, "High spectral efficiency DWDM-PON using an optical homodyne receiver with integral circuits based on digital signal processing," in *Proc. Opt. Fiber Commun. Conf.*, San Diego, CA, 2008, paper OTuH7.

[5] M. Gregory, F. Heine, H. Kaempfner, R. Lange, K. Saucke, U. Sterr, and R. Meyer, "Inter-satellite and satellite-ground laser communication links based on homodyne BPSK," in *Proc. SPIE 7587, 75870E*, Jan. 2010.

[6] B. Smutny, H. Kaempfner, G. Muehlnikel, U. Sterr, B. Wandernoth, F. Heine, U. Hildebrand, D. Dallmann, M. Reinhardt, A. Freier, R. Lange, K. Boehmer, T. Feldhaus, J. Mueller, A. Weichert, P. Greulich, S. Seel, R. Meyer, and R. Czichy, "5.6 Gbps optical intersatellite communication link," in *Proc. SPIE (Free-Space Laser Communication Technologies XXI)*, Aug. 2009, vol. 7199, pp. 719906–719906.

[7] M. Toyoshima, Y. Takayama, T. Takahashi, K. Suzuki, S. Kimura, K. Takizawa, T. Kuri, W. Klaus, M. Toyoda, and H. Kunimori, "Ground-to-satellite laser communication experiments," *IEEE Aerosp. Electron. Syst. Mag.*, vol. 23, no. 8, pp. 10–18, Aug. 2008.

[8] M. Toyoshima, H. Takenaka, and Y. Takayama, "Atmospheric turbulence-induced fading channel model for space-to-ground laser communications links," *Opt. Exp.*, vol. 19, pp. 15965–15975, Aug. 2011.

[9] Y. Koyama, H. Kunimori, and Y. Takayama, "Optical amplifiers for space environment," in *Proc. ICSOS*, Feb. 2009, pp. 221–225.

[10] J. M. Kahn, "1 Gbit/s PSK homodyne transmission system using phase-locked semiconductor lasers," *IEEE Photon. Electron. Lett.*, vol. 1, no. 10, pp. 340–342, Oct. 1989.

[11] R. T. Ramos and A. J. Seeds, "Fast heterodyne optical phase-lock loop using double quantum well laser diodes," *Electron. Lett.*, vol. 28, no. 1, pp. 82–83, 1992.

[12] U. Gliese, N. T. Nielsen, M. Bruun, E. L. Christensen, K. E. Stubkjaer, S. Lindgren, and B. Broberg, "A wideband heterodyne optical phase-locked loop for generation of 3–18 GHz microwave carriers," *IEEE Photon. Technol. Lett.*, vol. 4, no. 8, pp. 936–938, Aug. 1992.

[13] S. Kobayashi and T. Kimura, "Coherence of injection phase-locked AlGaAs semiconductor laser," *Electron. Lett.*, vol. 16, no. 7, pp. 668–670, 1980.

[14] R. Hui, A. D'Ottavi, A. Mecozzi, and P. Spano, "Injection locking in distributed feedback semiconductor lasers," *IEEE J. Quantum Electron*, vol. 27, no. 6, pp. 1688–1695, Jun. 1991.

[15] O. Lidoyne, P. Gallion, C. Chabran, and G. Debarge, "Locking range, phase noise and power spectrum of an injection-locked semiconductor laser," *Proc. Inst. Elec. Eng.*, vol. 137, no. 3, pp. 147–154, 1990, pt. J.

[16] M. G. Taylor, "Coherent detection method using DSP for demodulation of signal and subsequent equalization of propagation impairments," *IEEE Photon. Technol. Lett.*, vol. 16, no. 2, pp. 674–676, Feb. 2004.

[17] A. C. Bordonalli, C. Walton, and A. J. Seeds, "High-performance phase locking of wide linewidth semiconductor lasers by combined use of optical injection and optical phase-lock loop," *J. Lightw. Technol.*, vol. 17, no. 2, pp. 328–342, Feb. 1999.

[18] R. T. Ramos, P. Gallion, D. Erasme, A. J. Seeds, and A. Bordonalli, "Optical injection locking and phase-lock loop combined systems," *Opt. Lett.*, vol. 19, no. 1, pp. 4–6, Jan. 1994.

[19] M. J. Fice and A. J. Seeds, "Frequency-selective homodyne coherent receiver with an optical injection phase lock loop," *Proc. OFC/NFOEC*, Feb. 2008, paper OWT1.

[20] M. J. Fice, A. J. Seeds, B. J. Pugh, J. M. Heaton, and S. J. Clements, "Homodyne coherent receiver with phase locking to orthogonal-polarization pilot carrier by optical injection phase lock loop," *Proc. OFC/NFOEC*, Mar. 2009, paper OTuG1.

[21] M. J. Fice, A. Chiuchiarelli, E. Ciaramella, and A. J. Seeds, "Homodyne coherent optical receiver using an optical injection phase-lock loop," *J. Lightw. Technol.*, vol. 29, no. 8, pp. 1152–1164, Apr. 2011.

[22] C. C. Renaud, M. Duser, C. F. C. Silva, B. Puttnam, T. Lovell, P. Bayvel, and A. J. Seeds, "Nanosecond channel-switching exact optical frequency synthesizer using an optical injection phase-locked loop (OIPLL)," *IEEE Photon. Technol. Lett.*, vol. 16, no. 3, pp. 903–905, Mar. 2004.

[23] Y. Shoji, M. J. Fice, Y. Takayama, M. Toyoshima, and A. J. Seeds, "Feasibility study of coherent LEO-Ground link system using an optical injection phase lock loop technique," in *Proc. IEEE Int. Conf. Space Opt. Syst. Applications*, May 2011.

[24] S. Arnon, "Power versus stabilization for laser satellite communication," *Appl. Opt.*, vol. 38, no. 15, pp. 3229–3233, May 1999.

[25] D. Giggenbach, J. Horwath, and B. Epple, "Optical satellite downlinks to optical ground stations and high-altitude platforms," in *Proc. IST Mobile & Wireless Commun. Summit*, Budapest, Hungary, Jul. 2007, pp. 1–4.

[26] M. Toyoshima, H. Takenaka, Y. Shoji, Y. Takayama, Y. Koyama, and H. Kunimori, "Polarization measurements through space-to-ground atmospheric propagation paths by using a highly polarized laser source in space," *Opt. Exp.*, vol. 17, no. 25, pp. 22333–22340, Dec. 2009.

[27] X. Zou, X. Zhang, and C. Wen, "Research on bandwidth of optical filter in GEOLEO laser communication," in *Proc. 2nd Int. Conf. Biomed. Eng. Informat.*, Oct. 2009, pp. 1–4.

Yozo Shoji (S'98–M'99) received the B.E. and M.E. degrees in electrical engineering and Dr. Eng. degree in communications engineering from Osaka University, Osaka, Japan, in 1995, 1996, and 1999, respectively.

In 1999, he joined the Yokosuka Radio Communications Research Center, Communications Research Laboratory (CRL), Ministry of Posts and Telecommunications, Yokosuka, Japan, where he researched 60-GHz-band communications systems along with standardization activities for the frequency band in IEEE802.15.3c until 2007. In 2000, he invented a millimeter-wave self-heterodyne system and succeeded in a 60-GHz band wireless transmission of OFDM-based digital TV broadcast signals for the first time in the world. In 2008, he joined the Space Communications Group, National Institute of Information and Communications Technology (NICT) (formerly the Communications Research Laboratory), Tokyo, Japan, where he researched optical space communications systems and microwave photonics systems as a Senior Researcher. In 2010, he was awarded the Excellent Young Researchers Overseas Visit Program Fellowship by the Japan Society for the Promotion of Science (JSPS) and spent one year as a Visiting Researcher with the Photonics Group, Department of Electronic and Electrical Engineering, University College London (UCL), London, U.K., where he took part in research on coherent optical communications using an optical injection phase lock loop technique.

Dr. Shoji is a Senior Member of the Institute of Electrical, Information and Communication Engineers (IEICE), Japan. He was the recipient of the IEICE Young Researchers Award (2000), CRL Excellent Achievement Award (2003), IEICE Communications Society: Distinguished Contributions Award (2006), IEICE Electronics Society: Electronics Society Award (2007), Young Scientists Prize in the Commendation for Science and Technology by the Minister of Education, Culture, Sports, Science and Technology (2008), and the Meritorious Award on Radio by the Association of Radio Industries and Businesses (ARIB) (2010).

Martyn J. Fice (S'86–M'87) received the B.A. degree in electrical sciences and Ph.D. degree in microelectronics from the University of Cambridge, Cambridge, U.K., in 1984 and 1989, respectively.

In 1989, he joined STC Technology Laboratories, Harlow, U.K. (later acquired by Nortel), where he was engaged for several years in the design and development of InP-based semiconductor lasers for undersea optical systems and other applications. Subsequent work at Nortel involved research into various aspects of optical communications systems and networks, including wavelength-division multiplexing, all-optical wavelength conversion, optical regeneration, and optical packet switching. Since 2005, he has been a Senior Research Fellow with the Photonics Group, Department of Electronic and Electrical Engineering, University College London, London, U.K. His current research interests include optical transmission systems, coherent optical detection, optical phase-lock-loop techniques, and millimeter and THz wave generation and detection.

Dr. Fice is a member of the Institution of Engineering and Technology and a Chartered Engineer.

Yoshihisa Takayama received the Ph.D. degree from Hokkaido University, Sapporo, Japan, in 1998.

He then joined the National Institute of lnfbrmation Communications Technology (NICT) (formerly Communications Research Laboratory), Japan in 1999. He joined the Japan Aerospace Exploration Agency (JAXA) in 2004 to conduct satellite laser communication demonstrations and returned to NICT in 2007. His current research interests are phase conjugate optics, photonic crystals, computational electromagnetics, and free-space laser communications.

Alwyn J. Seeds (M'81–SM'92–F'97) received the Ph.D. and D.Sc. degrees from the University of London, London, U.K.

He was a Staff Member with Lincoln Laboratory, Massachusetts Institute of Technology, Cambridge, where he was involved in research on millimeter-wave GaAs integrated circuits. In 1986, he joined University College London, London, U.K., where he is currently a Professor of Optoelectronics and Head of the Department of Electronic and Electrical Engineering. He is a cofounder of Zinwave, a manufacturer of wireless over fiber systems.

Prof. Seeds is a Fellow of the Royal Academy of Engineering (U.K.).